

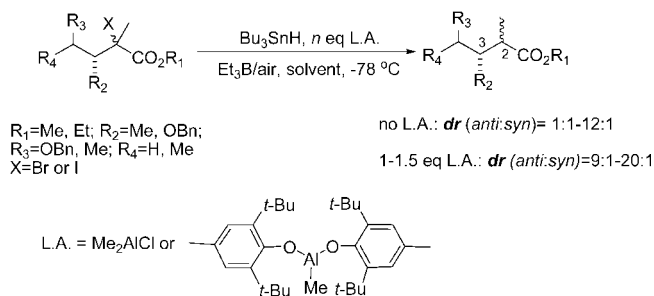
# Raising the Ceiling of Diastereoselectivity in Hydrogen Transfer on Acyclic Radicals

Irina Denissova,<sup>†</sup> Luca Maretti,<sup>||</sup> Brian C. Wilkes,<sup>†</sup> J.C. Scaiano,<sup>||</sup> and Yvan Guindon<sup>\*,‡,§</sup>

*Institut de Recherches Cliniques de Montréal (IRCM), 110 avenue des Pins Ouest, Montréal, Québec, Canada H2W 1R7, Department of Chemistry, Université de Montréal, C.P.6128, succursale Centre-ville, Montréal, Québec, Canada H3C 3J7, Department of Chemistry, McGill University, 801 rue Sherbrooke Ouest, Montréal, Québec, Canada H3A 2K6, and Department of Chemistry, University of Ottawa, 10 Marie Curie, Ottawa, Ontario, Canada K1N 6N5*

yvan.guindon@ircm.qc.ca

Received November 30, 2008



We report here that the monodentate complexation of  $\text{Me}_2\text{AlCl}$  to an ester group significantly enhances the selectivity of hydrogen transfer on acyclic radicals flanked by both an ester functionality and a stereogenic center, leading to C-2,C-3-*anti* products with high diastereoselectivity. In certain cases improved ratios were obtained using bulkier aluminum Lewis acid such as MAD (methylaluminum-di(di-2,6-*tert*-butyl-4-methylphenoxide)). Electron spin resonance studies on these acyclic radicals indicate that Lewis acid complexation leads to conformational changes in the radicals. The stereochemistry of the preferred enolate radicals complexed with Lewis acids and their impact on the acyclic transition states involved are suggested.

## Introduction

Many natural products of significant biological interest (e.g., polyketides) contain an acyclic subunit, consisting of a defined sequence of stereogenic centers with various chemical functionalities, synthesis of which is often very problematic. Indeed, inducing stereoselectivity in reactions involving acyclic molecules poses a significant challenge due to their high flexibility, allowing for multiple transition states of similar energy and poor stereoselectivity. The use of a Lewis acid can significantly improve the selectivity either by restricting the number of conformations via temporary ring formation or by changing the steric and stereoelectronic factors around the site being transformed, thus favoring one transition state. Since the early 1990s Lewis acids have been widely employed to improve the

diastereoselectivity of processes involving radical intermediates.<sup>1</sup> Our group has studied extensively the influence of Lewis acids on the reactivity of tertiary acyclic radicals flanked both by an ester and a stereocenter at C-3 in hydrogen transfer and allylation reactions.<sup>2</sup> These radicals are formed by the homolytic cleavage of either a carbon–halogen or a carbon–selenium bond of the corresponding  $\alpha$ -halo or seleno-esters. The relative stereochemistry varies depending on the reaction conditions used. Thus, the C-2,C-3-*syn* products are obtained when the hydrogen transfer reactions are conducted in the presence of bidentate Lewis acid (the *endocyclic* effect) as illustrated in Scheme 1

(1) For the most recent review, see: Guérin, B.; Ogilvie, W. W.; Guindon, Y. *Lewis Acid-Mediated Diastereoselective Radical Reactions*. In *Radicals in Organic Synthesis*; VCH: Weinheim, 2001; Vol. 1, pp 441–460.

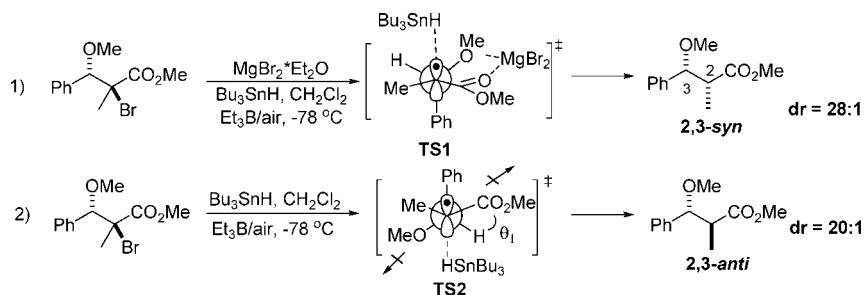
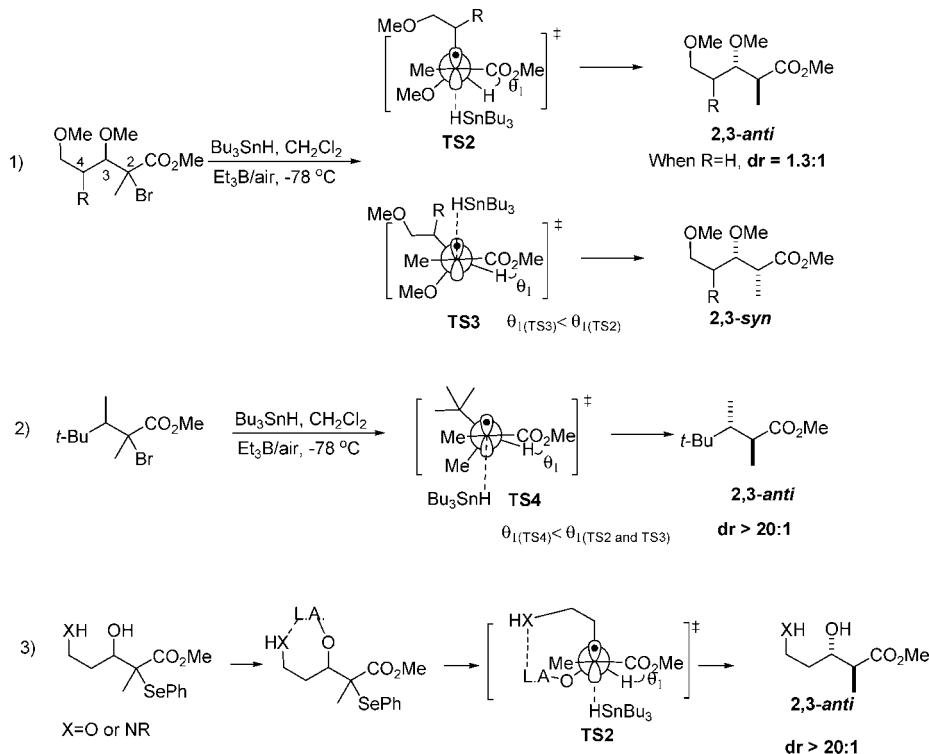
(2) (a) Cardinal-David, B.; Brazeau, J.-F.; Katsoulis, I.; Guindon, Y. *Curr. Org. Chem.* **2006**, *10*, 1939–1961. (b) Guérin, B.; Chabot, C.; Mackintosh, N.; Ogilvie, W. W.; Guindon, Y. *Can. J. Chem.* **2000**, *78*, 852–867. (c) Guindon, Y.; Jung, G.; Guérin, B.; Ogilvie, W. W. *Synlett* **1998**, *3*, 213–220. (d) Guindon, Y.; Guérin, B.; Rancourt, J.; Chabot, C.; Mackintosh, N.; Ogilvie, W. W. *Pure Appl. Chem.* **1996**, *68*, 89–96.

<sup>†</sup> Institut de Recherches Cliniques de Montréal.

<sup>‡</sup> Université de Montréal.

<sup>§</sup> McGill University.

<sup>||</sup> University of Ottawa.

SCHEME 1. Proposed Transition States Leading to the Corresponding 2,3-*syn* and 2,3-*anti* ProductsSCHEME 2. Proposed Transition States for Substrates Not Having a Disubstituted C-4 Center and without a  $\beta$ -Heteroatom

(entry 1).<sup>3</sup> When no Lewis acid is added, C-2,C-3-*anti* diastereomers are generated (entry 2).<sup>4</sup>

The lowest energy transition states **TS1** and **TS2** were proposed to rationalize the major products obtained in these reactions. The *anti*-diastereoselectivity noted in the latter case was dependent on the presence of an ester (or amide) at C-1 and maximized by the presence of a heteroatom at C-3. A substituent at C-4 (R) was also found to be critical, a lower ratio being observed when  $\text{R} = \text{H}$  (entry 1, Scheme 2).

In kinetically controlled reactions, such as the hydrogen transfer reaction in this study, the ratio of observed products is determined by the difference of energy between the corresponding transition states leading to the *anti* and *syn* products (**TS2** versus **TS3**). **TS2**, the lowest energy transition state, is the result of the synergy between steric and electronic factors: the minimization of the allylic-1,3 strain and of the intramolecular

dipole–dipole repulsion. As suggested before,<sup>5</sup> this leads to the dihedral angle  $\theta_{1(\text{TS2})}$  being close to  $30^\circ$ . The top face attack, leading to the *syn* product, imposes the  $\theta_1$  of **TS3** to be smaller than  $\theta_1$  in **TS2**. The dipole–dipole repulsion is not completely minimized in **TS3**, increasing the energy of the transition state. Moreover, the trajectory of the incoming hydrogen donor would be more sterically encumbered in **TS3** than in **TS2**, increasing even more the difference in energy between these transition states. When  $\text{R} = \text{H}$ , this difference is decreased as reflected by lower ratios.

In the absence of the heteroatom at C-3 and thus of dipole–dipole repulsion, the minimization of 1,3-allylic strain then becomes the major controlling factor (Scheme 2, entry 2). It favors the conformation in which the  $\beta$ -hydrogen is placed in the plane with the ester bringing the dihedral angle  $\theta_1$  close to  $0^\circ$ . Thus, the dihedral angle  $\theta_1$  in **TS4** is smaller than  $\theta_1$  in both **TS2** and **TS3**. As a result, significant *anti*-ratios in these cases could only be achieved in the presence of a very bulky

(3) (a) Guindon, Y.; Rancourt, J. *J. Org. Chem.* **1998**, *63*, 6554–6565. (b) Guindon, Y.; Guérin, B.; Chabot, C.; Ogilvie, W. W. *J. Am. Chem. Soc.* **1996**, *118*, 12528–12535. (c) Guindon, Y.; Lavalée, J.-F.; Llinas-Brunet, M.; Horner, G.; Rancourt, J. *J. Am. Chem. Soc.* **1991**, *113*, 9701–9702.

(4) (a) Guindon, Y.; Lavalée, J.-F.; Boisvert, L.; Chabot, C.; Delorme, D.; Yoakim, C.; Hall, D.; Lemieux, R.; Simoneau, B. *Tetrahedron Lett.* **1991**, *32*, 27–30. (b) Guindon, Y.; Yoakim, C.; Lemieux, R.; Boisvert, L.; Delorme, D.; Lavalée, J.-F. *Tetrahedron Lett.* **1990**, *31*, 2845–2848.

(5) Giese, B.; Damm, W.; Wetterich, F.; Zeic, H.-G.; Rancourt, J.; Guindon, Y. *Tetrahedron Lett.* **1993**, *34*, 5885–5888.

(6) (a) Giese, B.; Damm, W.; Wetterich, F.; Zeic, H.-G. *Tetrahedron Lett.* **1992**, *33*, 1863–1862. (b) Durkin, K.; Liotta, D.; Rancourt, J.; Lavalée, J.-F.; Boisvert, L.; Guindon, Y. *J. Am. Chem. Soc.* **1992**, *114*, 4912–4914.

substituent (e.g., *t*-Bu group).<sup>6</sup> These steric requirements, unfortunately, severely restrict the synthetic usefulness of these hydrogen transfer reactions, and the search for solutions has become an objective.

In the past we reported that linking the substituent at C-3 and C-5 through a ring (the *exo*-cyclic effect)<sup>7</sup> is a strategy that could be used to circumvent some of these problems (where R = H) as seen in entry 3, Scheme 2. The present study offers another solution. Herein we report that the formation of a monodentate complex with the ester group, using a bulky aluminum Lewis acid, can significantly improve the hydrogen transfer diastereoselectivity.<sup>8</sup> A mechanistic rationale, supported by electron spin resonance (ESR) studies, is suggested.

## Results and Discussion

We have observed an increase in *anti*-diastereoselectivity and in relative rates of the hydrogen transfer when studying the radical reduction of various  $\beta$ -alkoxy- $\alpha$ -halo-esters<sup>9</sup> with Bu<sub>3</sub>SnH and Lewis acid in dichloromethane (DCM) or toluene at  $-78^\circ\text{C}$  (Table 1).

As shown in Table 1 (entries 1–3), a significant increase of diastereomeric *anti:syn* ratio going from 10:1 to 20:1 was observed in the reduction of ester **1** when 1.0 equiv of Me<sub>2</sub>AlCl was added. The yields were also improved. One will note that the time needed to complete the reaction was significantly reduced (from 6 to 1 h). Studying the radical reduction of the  $\beta$ -alkoxy ester not having a tertiary carbon center at C-4 (a disubstituted carbon center) such as **4** was also of great interest. Not surprisingly, its reaction in the absence of Lewis acid gave almost no diastereoselectivity (entries 4 and 5) in both DCM and toluene. Remarkably, almost a 3-fold increase of diastereoselectivity was noted in the presence of 1.0 equiv of Me<sub>2</sub>AlCl in toluene, the ratio rising from 1.5:1 to 4:1 (entry 6). This ratio was further improved to 6.5:1 by replacing Me<sub>2</sub>AlCl with a bulkier aluminum Lewis acid such as MAD (methylaluminum-di(di-2,6-*tert*-butyl-4-methylphenoxide), Figure 1)<sup>10,11</sup> in toluene (entry 7). A ratio of 9:1 was obtained when 4 equiv of MAD was used (entry 8). No reaction was observed in the absence of the initiator (Et<sub>3</sub>B) (entry 9), attesting to the involvement of a free-radical-based process in the reactions previously described (vide supra).

We then turned our attention to substrates lacking the alkoxy group at C-3 and therefore dependent solely on steric factors in their hydrogen transfer reactions. In the absence of the Lewis acid the reduction of a C-2,C-3 diastereomeric mixture of  $\alpha$ -iodo- $\beta$ -methyl-esters **7** and **8** gave a 12:1 selectivity favoring the *anti*-diastereomer (entry 10). This result is extremely

interesting in its own right, suggesting that a combination of a tertiary centered free radical, an ester, and a sequence of contiguous tertiary carbon centers maybe sufficient to foster diastereoselectivity. A mixture of side products **11** and **12** resulting from the oxygen addition was also isolated in 20% yield. When the reaction was performed using either 1.5 equiv of Me<sub>2</sub>AlCl in toluene (entry 11) or employing a larger excess of Me<sub>2</sub>AlCl in CH<sub>2</sub>Cl<sub>2</sub> (entry 12), the *anti:syn* product ratio increased to >20:1. The formation of the side product was also suppressed.

Aryl ester **13** was studied next. Unsurprisingly, for this ester having an sp<sup>2</sup> carbon center at C-4, the diastereoselectivity of the hydrogen transfer reaction in the absence of the Lewis acid was low in both DCM and toluene (3:1 and 2.3:1 respectively, entries 13 and 14). Adding 1.5 equiv of MAD in toluene improved the diastereoselectivity by 2-fold, a 6:1 ratio being obtained (entry 15). *Collectively, these results underline the utility of aluminum Lewis acids in enhancing the diastereoselectivity of the hydrogen transfer even in case of “problematic” substrates.* A mechanistic rationale was then sought.

**Mechanistic Considerations.** Upon addition of Me<sub>2</sub>AlCl to  $\beta$ -alkoxy-esters, complexes **16** and **17** between the Lewis acid and the substrate may be formed (Scheme 3).

These complexes are in equilibrium with the noncomplexed substrate. Complex **18** could also be formed.<sup>12–14</sup> One will note that (as illustrated in Scheme 1, entry 1) bidentate complexes (**17** or **18**) should lead to *syn* products as the result of hydrogen transfer reaction. However, in our experiments (using 1 equiv of Me<sub>2</sub>AlCl) we have observed an improvement of the ratios favoring the *anti* isomer, suggesting empirically that the bidentate reaction pathways were neither dominant nor important.

We decided to verify qualitatively the nature of the complexes induced by Me<sub>2</sub>AlCl and the substrate in solution using <sup>13</sup>C NMR (Figure 2A–C).

The <sup>13</sup>C NMR performed on ester **1** with 1 equiv of Me<sub>2</sub>AlCl in CD<sub>2</sub>Cl<sub>2</sub> at  $-40^\circ\text{C}$  points in the direction of the formation of a monodentate carbonyl–Me<sub>2</sub>AlCl complex as the most populated intermediate (Figure 2B). Indeed, there is a downfield shift of the signal belonging to the ester quaternary carbon accompanied by a significant line-broadening of this peak. Line-broadening suggests a dynamic equilibrium between the carbonyl–Me<sub>2</sub>AlCl complex and the free carbonyl group.<sup>15</sup> The methyl of the ester is also shifted downfield ( $\Delta\delta = 4.7$  ppm). Remarkably, the <sup>13</sup>C NMR of ester **1** with 4 equiv of Me<sub>2</sub>AlCl at  $-40^\circ\text{C}$  (Figure 2C) reveals the formation of a distinct new species, the signals of the ester, methyne (C-3), and benzylic methylene carbons having shifted downfield with  $\Delta\delta = 11.7$ , 7.2, and 8.1 ppm, respectively. This new species was identified as bidentate ionic complex **19** (Scheme 4). To our knowledge, this is a first observation of such a complex for  $\beta$ -alkoxy esters.

Additional experimental evidence of the bidentate complex formation was obtained from the radical reduction of ester **1** in the presence of 4 equiv of Me<sub>2</sub>AlCl in DCM at  $-78^\circ\text{C}$  (Scheme

(7) (a) Guindon, Y.; Prévost, M.; Mochirian, P.; Guérin, B. *Org. Lett.* **2002**, *4*, 1019–1022. (b) Guindon, Y.; Liu, Z.; Jung, G. *J. Am. Chem. Soc.* **1997**, *119*, 9289–9290. (c) Guindon, Y.; Faucher, A.-M.; Bourque, E.; Caron, V.; Jung, G.; Landry, S. *J. Org. Chem.* **1997**, *62*, 9276–9283.

(8) There are only few examples in the literature where the use of monodentate chelates between the carbonyl and the Lewis acid influences the diastereoselectivity of either a radical reduction or an atom transfer on the radicals. For example, Sato et al. reported that using a bulky aluminum Lewis acid such as methylaluminum di(2,4,6-trimethylphenoxide) in the radical addition of BuI to  $\alpha$ -methelene- $\gamma$ -phenyl-butylolactone in the presence of Bu<sub>3</sub>SnH reversed the selectivity of the hydrogen-transfer step, favoring formation of *anti* product (dr = 1.5:1), whereas in the absence of the Lewis acid good *syn*-selectivity (dr = 9:1) was observed. See: Urabe, H.; Kobayashi, K.; Sato, E. *J. Chem. Soc. Chem. Commun.* **1995**, *104*, 3–1044.

(9) The preparation of the esters is described in Supporting Information.

(10) Maruoka, K.; Itoh, T.; Sakurai, M.; Nonoshita, K.; Yamamoto, H. *J. Am. Chem. Soc.* **1988**, *110*, 3588–3597.

(11) Renaud, P.; Moufid, N.; Kuo, L. H.; Curran, D. P. *J. Org. Chem.* **1994**, *59*, 3547–3552.

(12) Previous studies in the literature have demonstrated formation of monodentate complexes **16** when 1 equiv of Me<sub>2</sub>AlCl was added to  $\beta$ -alkoxy-aldehydes,  $\beta$ -alkoxy-ketones (see ref 13), and  $\beta$ -alkoxy-oxazolodinones (see ref 14), whereas using an excess of the Lewis Acid led to formation of bidentate ionic complexes **18**.

(13) Evans, D. A.; Allison, B. D.; Yang, M. G.; Masse, C. E. *J. Am. Chem. Soc.* **2001**, *123*, 10840–10852.

(14) Castellino, S.; Dwight, W. J. *J. Am. Chem. Soc.* **1993**, *115*, 2986–2987.

(15) Castellino, S. *J. Org. Chem.* **1990**, *55*, 5197–5200, and ref 9 therein.

(16) We did also suggest in the past on the basis of the experimental data that the monodentate complexes reacted more rapidly than the bidentate complexes in the hydrogen-transfer reaction.

TABLE 1. Studies on the Radical Reduction

Entry	L.A. (equiv)	Reaction Time	Solvent	dr (2,3- <i>anti</i> : <i>syn</i> )	Yield (%)
1	-	6 h	DCM	10:1	50 <sup>a</sup>
2	Me <sub>2</sub> AlCl (1.0)	1 h	DCM	16:1	90
3	Me <sub>2</sub> AlCl (1.0)	1 h	toluene	20:1	100
4	-	4 h	DCM	1:1	100 <sup>b</sup>
5	-	1 h 25 min	toluene	1.5:1	96
6	Me <sub>2</sub> AlCl (1.0)	1 h 30 min	toluene	4:1	71
7	MAD (1.5)	1 h	toluene	6.5:1	79
8	MAD (4.0)	1 h	toluene	9:1	68
9 <sup>c</sup>	MAD (1.5)	2 h 30 min	toluene	no reaction	-
10	-	40 min	DCM	12:1	73
11	Me <sub>2</sub> AlCl (1.5)	10 min	toluene	20:1	100
12	Me <sub>2</sub> AlCl (4.0)	10 min	DCM	> 20:1	80
13	-	1 h	DCM	3:1	95
14	-	1 h	toluene	2.3:1	89
15	MAD (1.5)	1 h	toluene	5:1 to 6.5:1	78

<sup>a</sup> Reaction did not go to completion; ~50% starting material was still present. <sup>b</sup> Conversion based on <sup>1</sup>H NMR of the crude. <sup>c</sup> No Et<sub>3</sub>B was added.

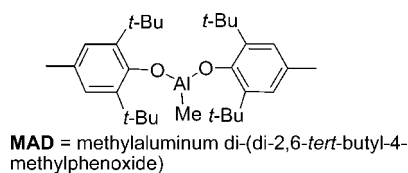
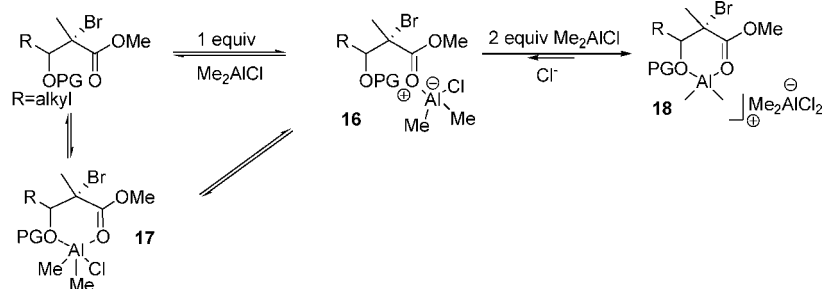


FIGURE 1. Structure of MAD.

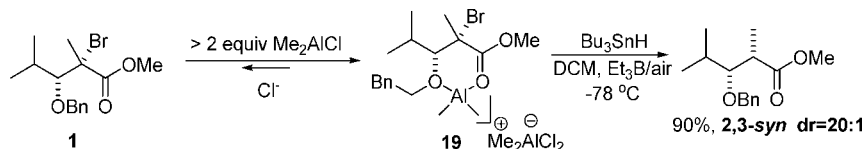
4, step 2). The reaction afforded *syn* diastereomer in 20:1 ratio, signifying involvement of bidentate transition state **TSI** (Scheme 1, entry 1). One may thus conclude that only the monodentate

pathway is operative in the hydrogen transfer when 1 equiv of Me<sub>2</sub>AlCl is used.<sup>16</sup>

As shown in Scheme 5 complex **20** and the nonchelated ester could both participate in the formation of the carbon-centered radical via halogen abstraction and the subsequent hydrogen transfer reaction. Hence, in the case of the hydrogen transfer reaction, responsible for a diastereoselective outcome, four competing pathways are possible, as illustrated in Scheme 5. Two transition states **A** (nonchelated) and **C** (monochelated) would lead to the *anti* product, while the corresponding **B** (nonchelated) and **D** (monochelated) lead to *syn* products.

SCHEME 3. Formation of Mono- and Bidentate Complexes between the Ester and Me<sub>2</sub>AlCl

## SCHEME 4. Formation of Bidentate Ionic Complex 19 Followed by the Hydrogen Transfer Reaction



We believe that transition states **C** and **D** are lower in energy than their corresponding nonchelated versions. Indeed, the presence of an electron-withdrawing group  $\alpha$  to a carbon-centered radical is known to increase its reactivity toward trialkyltin hydrides.<sup>17</sup> A complexation of an ester by a Lewis acid would enhance the electron-withdrawing characteristics of this functionality. In other words, the complexation of the Lewis acid to the ester is expected to lower the radical SOMO energy, thus allowing for a better overlap with the HOMO energy of Bu<sub>3</sub>SnH, which will decrease the energy of the transition states. A similar argument would suggest that the halogen abstraction step (by the electropositive tin radical) also accelerates when the ester becomes more electrophilic upon coordination with a Lewis acid.<sup>18</sup> Taken together, this should result in the increase of the relative reaction rates, which indeed was observed in our studies from reduced reaction times in cases when Me<sub>2</sub>AlCl was used.

However this would not explain per se an increase in the *anti*-preferred ratio, since both the *syn*- and the *anti*-predictive transition states would be lowered upon complexation with Me<sub>2</sub>AlCl. Such an increase could only be explained if the difference of energy between **C** and **D** (complexed transition states) is greater than between **A** and **B** (noncomplexed transition states).

What are the factors at the origin of the increase in energy difference between transition states **C** and **D** as compared to the one between **A** and **B**? One hypothesis would be to postulate a *conformational change* of the complexed free radicals in the transition state rendering the addition from the top face more difficult. As suggested by Fischer and others, a carbon-centered free radical  $\alpha$  to the ester is planar and could therefore exhibit an enol-like character.<sup>19</sup> Hence, such an enol-like radical can exist in the two geometrical forms **Z** (**21**) and **E** (**22**) (Scheme 6, entry 1).

Recently, Spichty et al. have reported UB3LYP/6-31G\* calculations of the minimum geometry of [D<sub>3</sub>]methyl-2-methyl-4,4,4-trichlorobutanoate-2-yl radical.<sup>20</sup> The *E*-isomer was found to be 0.33 kcal/mol more stable than the corresponding *Z*-isomer. Moreover, values for the dihedral angle of  $\theta_{1(E\text{-isomer})} = 15.9^\circ$  and  $\theta_{1(Z\text{-isomer})} = 18.0^\circ$  were obtained. One could attribute the angle increase to the increased 1,3-allylic strain in the *Z*-isomer as compared to the *E*-isomer (OR > O'). The situation may be different in our case, the oxygen radical being complexed with a sterically demanding Lewis acid. In the isomer **E** (**23**) (note change of ordering priority due to complexing L.A.) strong 1,2-interaction is now present, whereas in the *Z*-isomer (**24**) the allylic 1,3-strain is further increased (Scheme 6, entry 2). What will be the net directing effect of such complexation on the equilibrium between *E*- and *Z*-isomers?

To address this question, theoretical calculations<sup>21</sup> were performed on model olefins **25-Z** and **26-E** (Figure 3, entry 1) and **25'-Z** and **26'-E** where a *tert*-butyl group replaced the Lewis

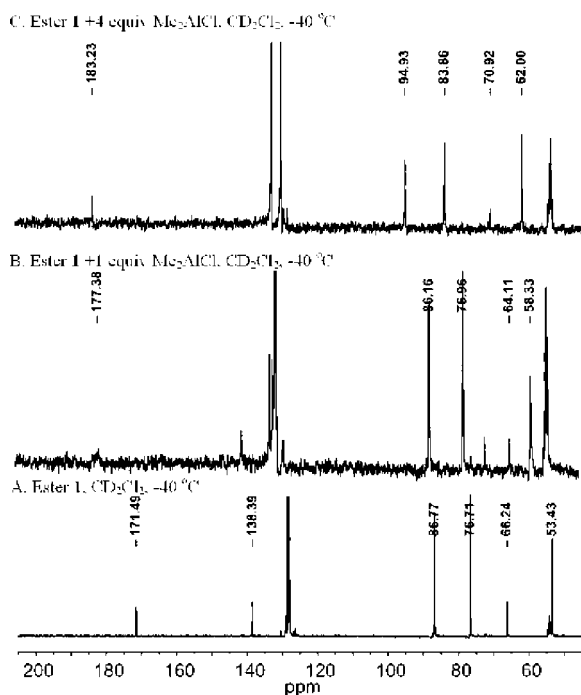


**FIGURE 2.** <sup>13</sup>C NMR of ester **1** with 0.0 (A), 1.0 equiv (B), and 4.0 equiv (C) of Me<sub>2</sub>AlCl recorded at -40 °C.

(17) Avila, D. V.; Ingold, K. U.; Luszytk, J.; Dolbier, W. R.; Pan, H. Q.; Muir, M. *J. Am. Chem. Soc.* **1994**, *116*, 99–104.

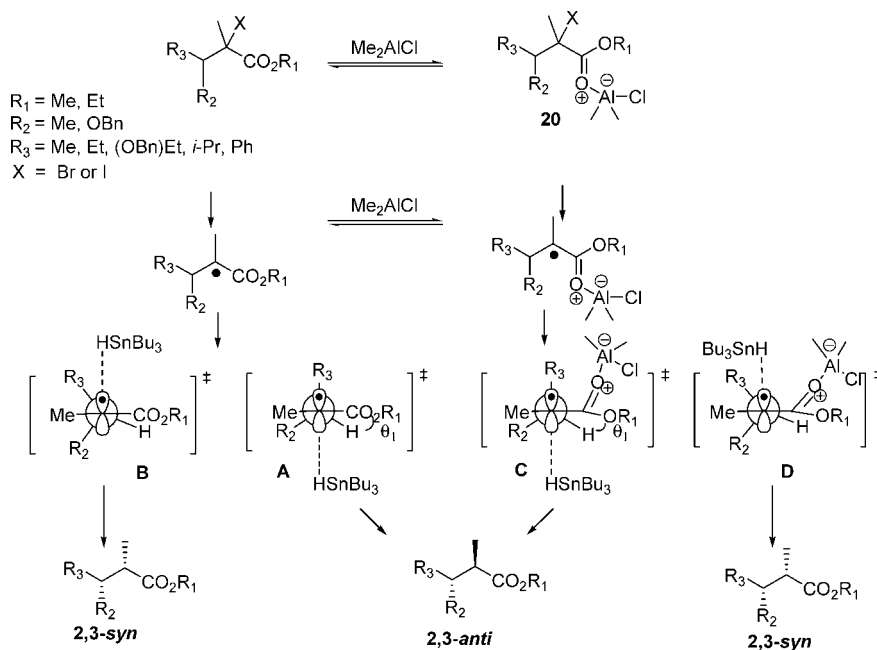
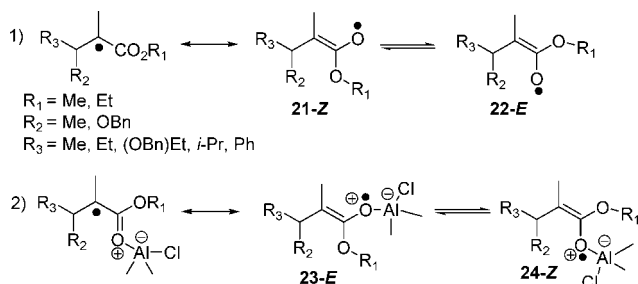
(18) (a) Xiao, X.; Pan, H.-Q.; Dolbier, W. R. *J. Am. Chem. Soc.* **1994**, *116*, 4521–4522. (b) Blackburn, E. V.; Tanner, D. D. *J. Am. Chem. Soc.* **1980**, *102*, 692–697. (c) Coats, D. A.; Tedder, J. M. *J. Chem. Soc., Perkin Trans. 2* **1973**, 1570–1574. (d) See also ref 3a.

(19) Roduner, E.; Strub, W.; Burkhard, P.; Hockmann, J.; Percival, P. W.; Fischer, H.; Ramos, M.; Webster, B. C. *Chem. Phys.* **1982**, *67*, 275–285.

(20) Spichty, M.; Giese, B.; Matsumoto, A.; Fischer, H.; Gescheidt, G. *Macromolecules* **2001**, *34*, 723–726.

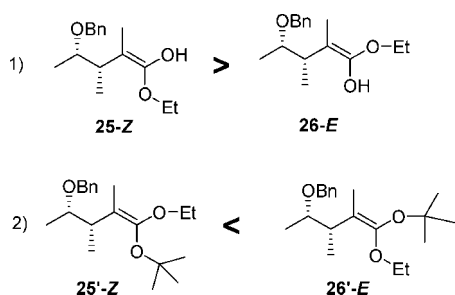


## SCHEME 5. Proposed Complexed and Noncomplexed Pathways for the Hydrogen Transfer

SCHEME 6. *Z* and *E* Enol Radicals with and without  $\text{Me}_2\text{AlCl}$ 

acid (Figure 3, entry 2). For the olefins without *tert*-butyl, the *E*-isomer was found to be 0.24 kcal/mol more stable than the *Z*-isomer, a value similar to the one reported by Spichty et al. for enolate-like  $[D_3]$ methyl-2-methyl-4,4,4-trichlorobutanoate-2-yl radical (vide supra). With the *tert*-butyl group added (**25'** and **26'**), the inverse was observed: the *Z*-isomer was found to be 1.46 kcal more stable than the *E*-isomer, suggesting that 1,2-allylic strain was more important than 1,3-allylic strain.

By analogy with the olefin model one could then conclude that the *Z*-enolate radical (**24**) (Figure 4) would be the prevalent specie involved in both the *anti*- (**C**) and *syn*-predictive (**D**) transition states of the hydrogen transfer. Importantly, this complexed *Z*-radical **24** would suffer from greater allylic 1,3-strain, which has to be alleviated, compared to noncomplexed **21** and **22**. This would therefore result in increase of the  $\theta_1$

FIGURE 3. Comparison of the **26-E** and **25-Z** enolates.

angle between the hydrogen at C-3 and the plane of the ester in **24**. This, in turn, would change the orientation of  $R_3$  and raise the energy of transition state **D** (Scheme 5), therefore increasing the energy difference between **C** and **D** as opposed to the one between **A** and **B**. (As discussed before, when  $R_2 = \text{OBn}$ , the minimization of the dipole–dipole electronic repulsion will further increase the  $\theta_1$  angle).

It is obviously difficult to experimentally support a hypothesis on an increased  $\theta_1$  angle in the transition state. However, the radicals being known to react through early transition states, the conformational changes in the ground state of these radicals may be reflected in the corresponding transition state. Thus we decided to study the conformational changes in the ground states of various radicals occurring upon complexation with  $\text{Me}_2\text{AlCl}$  with low-temperature ESR techniques.

The ESR spectrum of an acyclic radical represents averaged information obtained from a number of low energy conformations. Complexation with  $\text{Me}_2\text{AlCl}$  is expected to raise the rotation barriers (vide supra), the conformation with a larger dihedral angle becoming dominant. One should then detect an increase in the corresponding coupling constant.<sup>22</sup> The low-temperature ESR studies were performed on radicals **27–30** (Figure 5).

Indeed, in the presence of  $\text{Me}_2\text{AlCl}$  an increase in the  $\beta$ -hyperfine coupling constant with the proton at C3 was observed for both **29** and **30** compared to **27** and **28**, respectively, thus signifying increase in  $\theta_1$  upon complexation. The ESR experiments are described in the following section.

**ESR Experiments.** Nitrogen-equilibrated toluene solutions of halo-ester **1** or the mixture of **7** and **8** in the presence of  $\text{Me}_2\text{AlCl}$  (when applicable) and  $(\text{Bu}_3\text{Sn})_2$  were irradiated in the ESR spectrometer cavity at  $-78^\circ\text{C}$  (**7** and **8** mixture) and  $-40$

(21) See Experimental Section for details.

(22) These coupling constants are directly dependent on the  $\langle \cos^2 \theta_2 \rangle$ , where  $\theta_2$  is the dihedral angle formed by the direction of the  $2p_z$  axis (p orbital of the radical) and the direction of the corresponding C-H $\beta$  bond; the increase in the coupling constant reflects smaller angles between the p-orbital and the C-H $\beta$  bond. This means that the dihedral angle between this C-H $\beta$  bond and the plane of the ester increases ( $\theta_2 = 90^\circ - \theta_1$ ). See: Gerson, F.; Huber, W. *Electron Spin Resonance Spectroscopy of Organic Radicals*; VCH: Weinheim, 2003; p 61.

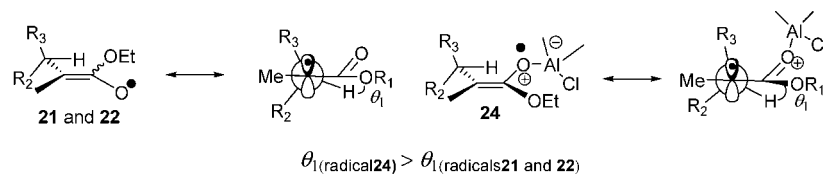


**FIGURE 4.** Increase of dihedral angle  $\theta_1$  occurring upon complexation of  $\text{Me}_2\text{AlCl}$ .

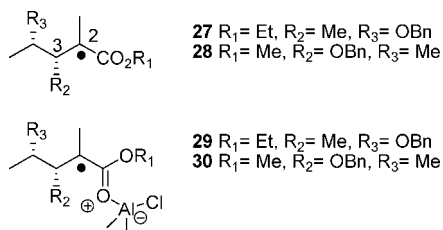


**FIGURE 5.** Series of radicals studied by ESR technique.

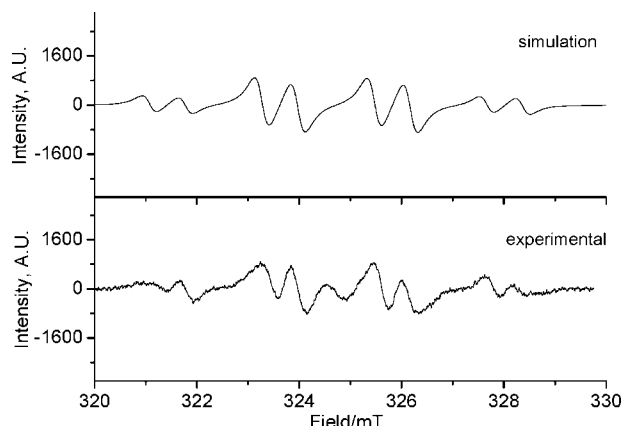


**FIGURE 6.** ESR spectrum of radical **27** (bottom) and its simulation (top).

$^{\circ}\text{C}$  (ester **1**).<sup>23</sup> Radicals were generated by continuous lamp irradiation upon  $(\text{Bu}_3\text{Sn})_2$  photolysis. As a control experiment, the ESR spectra were recorded for several minutes prior to lamp irradiation to ensure that radicals were not forming via any other pathway.

The ESR spectra of radicals **27** and **29** together with the spectra simulations<sup>24</sup> are shown on Figures 6 and 7, respectively. The ESR spectrum of radical **27** originating from esters **7** and **8** (Figure 6) features eight lines as expected from the coupling with the three equivalent protons of the methyl group at C-2 and the proton at C-3. Two coupling constants of 22.0 and 7.0 G for  $\text{CH}_3$  and  $\text{CH}$ , respectively, can be calculated from the spectrum. However, the intensity distribution slightly differs from that of expected binomial 1:1:3:3:3:3:1:1. This might indicate a coexistence of several low energy radical conformations with different  $\beta$ -hyperfine coupling constants. This makes it more difficult to explain the preference of the *anti* products in this series in the absence of the Lewis acid, which is reinforced by the fact that the spectrum of **27** does not exactly fit the simulation performed under assumption of a single conformation. Thus conformations **F**, **G**, and **H** could be populated in the ground state (Figure 8).

When the mixture of **7** and **8** is irradiated with  $\text{Me}_2\text{AlCl}$  in the solution, new radical species (presumably, radical **29**) with

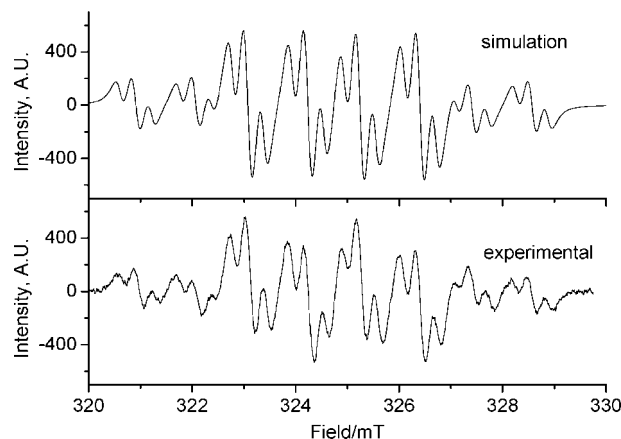


**FIGURE 7.** ESR spectrum of radical **29** (bottom) and its simulation (top).

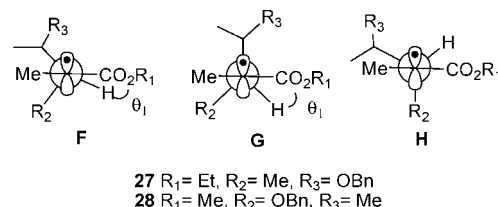


**FIGURE 8.** Possible low-energy ground-state conformations for radicals **27** and **28**.

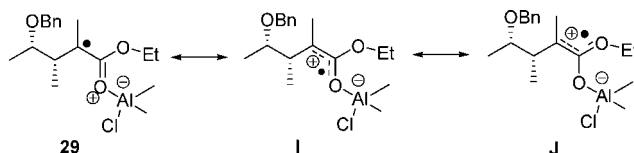


**FIGURE 9.** Possible resonance structures of radical **29**.

a distinctly different spectrum is detected (Figure 7). The  $\beta$ -coupling constant for the proton at C3 is now 11.5 G, which indicates significant changes in the conformation as well as an increase in dihedral angle  $\theta_1$ . There is also an additional smaller splitting with the coupling constant of 3.0 G. The coupling with the three protons of the methyl group remains the same (22.0 G). The simulation of the spectrum for radical **29** using these values gives the best overlap with the experimental spectrum when the additional splitting (3.0 G) arises from the coupling with two equivalent protons. These protons could come from the  $\text{CH}_2$  belonging to ethoxy group, indicating a full delocalization of the unpaired electron (Figure 9). It is reasonable to suggest that donation of the electron to form the delocalized structure should occur more readily from the most electron-rich oxygen thus making **J** (the Z-enol ether radical complex) a prevalent resonance structure. The  $g$ -value of 2.0045 calculated from the simulations also points to the delocalization of the unpaired electron on the oxygen. The spectrum of **29** fits well with simulation for a single conformation and thus could support the higher diastereoselectivity observed.

(23) See Experimental Section for further details.

(24) The computer simulations were performed using the EasySpin Software. See: Stoll, S.; Schweiger, A. *J. Magn. Reson.* **2006**, *178*, 42–55.

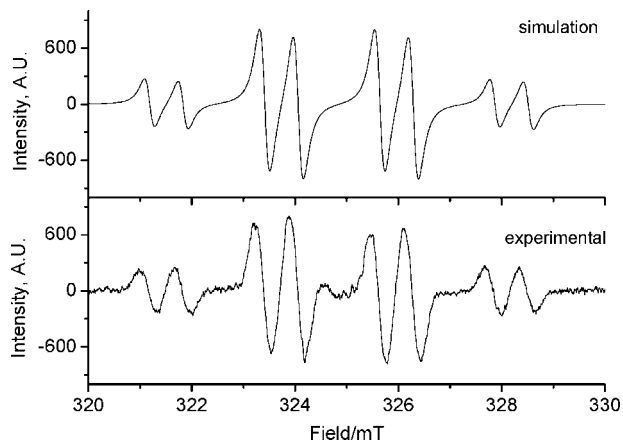


FIGURE 10. ESR spectrum of radical **28** (bottom) and its simulation (top).

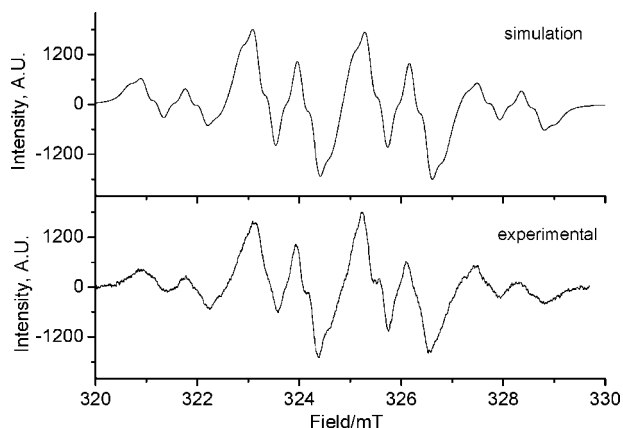


FIGURE 11. ESR spectrum of radical **30** (bottom) and its simulation (top).

The ESR spectrum of radical **28** (Figure 10) with  $\beta$ -coupling constants of 6.5 and 22.3 G exhibits the expected pattern with an appropriate binomial intensity distribution. This is consistent with the dual (minimization of allylic 1,3-strain and dipole–dipole repulsion) steric and electronic effects that have to be minimized to favor conformation **G** (Figure 8). When ester **1** is irradiated in the presence of  $\text{Me}_2\text{AlCl}$  to form radical **30**, a different spectrum is obtained (Figure 11). There is a line broadening and an increase in the second coupling constant to 8.5 G, also implying that changes in the conformation of the radical occur upon complexation of  $\text{Me}_2\text{AlCl}$  to the ester with an increase of the  $\theta_1$  angle. The broadening could be attributed to the poorly resolved third hyperfine coupling constant (resulting from the delocalization on the methyl ester) as well as to an existing dynamic equilibrium between complexed and noncomplexed radicals.

In conclusion, from comparison of the ESR spectra of radicals **27** and **28** (Figures 6 and 10, respectively), we suggest that when  $\text{R}_2 = \text{Me}$  (radical **27**), a larger number of low energy conformations is accessible than when  $\text{R}_2 = \text{OBn}$  (radical **28**) at the same temperature. When  $\text{Me}_2\text{AlCl}$  is added, the ESR spectra of **29** fits well the simulation for a single conformation, which could be at the origin of the increased diastereoselectivity of hydrogen transfer noted. In the case of **30** ( $\text{R}_2 = \text{OBn}$ ), a conformational preference is already established in the ground state, which angle  $\theta_1$  is further increased in the presence of  $\text{Me}_2\text{AlCl}$ .

## Conclusion

We have demonstrated that using either  $\text{Me}_2\text{AlCl}$  or a bulkier aluminum Lewis acid such as MAD can significantly enhance the diastereoselectivity of the hydrogen transfer reaction on acyclic radicals, thus expanding the scope of the previously developed methodology, which will certainly find further applications in synthesis. The low-temperature ESR studies confirmed that the complexation of the Lewis acid induces conformational changes in the radicals. This may be at the origin of the greater difference between relative energies of the corresponding *anti*- and *syn*-predictive transition states and therefore of the greater diastereoselectivity in the hydrogen transfer reaction.

## Experimental Section

**Theoretical Conformational Analysis.** All calculations were performed using the molecular modeling software SYBYL version 7.0 (Tripos Associates, St. Louis, MO). The standard Tripos force field<sup>25</sup> was used for energy calculations, and a dielectric constant of 78 was used. Molecules were constructed using the standard fragment library and were minimized using the conjugate gradient approach.<sup>26</sup> A grid search was performed on each compound in which the dihedral angles of all rotatable bonds were systematically varied by 30° increments.<sup>27</sup> For each search, the resulting conformers were grouped into families based on similarity of their dihedral angles ( $\pm 30^\circ$ ). The lowest energy member of each conformational family was then minimized extensively, and the resulting conformers were combined and ranked in order of increasing energy.

**ESR Measurements.** All measurements were carried out on a JEOL (FA 100) EPR spectrometer equipped with ES-DVT4 variable temperature controller. The 5-mm tube was placed into the cavity of the spectrometer and irradiated in situ by means of a Xenon illuminator (Luzchem). An  $\text{H}_2\text{O}$  infrared filter (10 cm in length) was placed between the lamp and the sample in order to avoid heating of the sample.

**Materials and Sample Preparation for the ESR Experiments.** Toluene (99.8%, anhydrous),  $\text{Me}_2\text{AlCl}$  (1 M solution in hexanes), and  $\text{Bu}_6\text{Sn}_2$  were purchased from Aldrich and used as supplied.

**A. Preparation of a Sample without  $\text{Me}_2\text{AlCl}$ .** A corresponding ester (1.00 mmol) was preweighed in a dry vial. To the vial was added toluene (500  $\mu\text{L}$ ), and the solution was transferred into the oven-dried tube. Then  $\text{Bu}_6\text{Sn}_2$  (50  $\mu\text{L}$ , 1.00 mmol) was added via syringe. The resulting solution was capped and degassed with  $\text{N}_2$  for at least 30 min.

**B. Preparation of a Sample with  $\text{Me}_2\text{AlCl}$ .** A corresponding ester (1.00 mmol) was preweighed in a flame-dried round-bottom flask and kept under  $\text{N}_2$  or argon. To the ester was added toluene ( $n$   $\mu\text{L}$ ). The flask was cooled with dry ice, followed by consequent addition of  $\text{Bu}_6\text{Sn}_2$  (50  $\mu\text{L}$ , 1.00 mmol) and  $\text{Me}_2\text{AlCl}$  ( $n$  mmol, 1 M in hexanes). [Quantities used: for ester **1**, toluene (400  $\mu\text{L}$ ),  $\text{Me}_2\text{AlCl}$  (100  $\mu\text{L}$ , 1.00 mmol); for the mixture of esters **7** and **8**, toluene (350  $\mu\text{L}$ ),  $\text{Me}_2\text{AlCl}$  (150  $\mu\text{L}$ , 1.50 mmol).] The resulting yellow solution was then quickly transferred via canula to the precooled (dry ice) flame-dried tube under  $\text{N}_2$ . (Alternatively, the tube can be dried in the oven at 140 °C for at least 2 h and cooled under  $\text{N}_2$  flow.) The solution was degassed with  $\text{N}_2$  for 20–30 min; the tube was kept in the beaker with dry ice at all times during the sample preparation.

(25) Clark, M.; Cramer, R.D. III; Opdenbosch, N. V. *J. Comput. Chem.* **1989**, *10*, 982–1012.

(26) Powell, M. J. D. *Math. Program.* **1977**, *12*, 241–254.

(27) (a) Wilkes, B. C.; Nguyen, T.M.-D.; Weltrowska, G.; Carpenter, K. A.; Lemieux, C.; Chung, N. N.; Schiller, P. W. *J. Peptide Res.* **1998**, *51*, 386–394. (b) Wilkes, B. C.; Schiller, P. W. *Biopolymers* **1995**, *37*, 391–400. (c) Wilkes, B. C.; Nguyen, T.M.-D.; Weltrowska, G.; Carpenter, K. A.; Lemieux, C.; Chung, N. N.; Schiller, P. W. *J. Peptide Res.* **1998**, *51*, 386–394.



**General Procedures for the Radical Reduction.** All diastereomeric ratios were determined from 500 MHz  $^1\text{H}$  NMR of the crude reaction mixture.

**A. Radical Reduction in the Absence of Lewis Acids.** To a solution of the ester (0.10 mmol) in  $\text{CH}_2\text{Cl}_2$  (1 mL) at  $-78^\circ\text{C}$  was added  $\text{Bu}_3\text{SnH}$  (54  $\mu\text{L}$ , 0.20 mmol) followed by addition of  $\text{Et}_3\text{B}$  (25  $\mu\text{L}$ , 0.025 mmol, 1 M in  $\text{CH}_2\text{Cl}_2$ ) and dry air (2 mL). Addition of  $\text{Et}_3\text{B}$ /air (25  $\mu\text{L}$ /2 mL) was repeated every 20 min, until reaction was judged completed by TLC. To the reaction mixture was then added *m*-dinitrobenzene, and the mixture was stirred for 15 min at  $-78^\circ\text{C}$ , followed by addition of brine and dilution with ether. The mixture was then warmed to rt, and the phases were separated. The aqueous phase was extracted with ether ( $\times 2$ ), and the combined organic fractions were dried over  $\text{MgSO}_4$  and concentrated under reduced pressure.

**B. Radical Reduction in the Presence of  $\text{Me}_2\text{AlCl}$ .** To a solution of the ester (0.10 mmol) in  $\text{CH}_2\text{Cl}_2$  or toluene (1 mL) at  $-78^\circ\text{C}$  was added  $\text{Me}_2\text{AlCl}$  (*n* equiv, 1 M in hexanes), stirred for 3–5 min. Then  $\text{Bu}_3\text{SnH}$  (54  $\mu\text{L}$ , 0.20 mmol) was added followed by addition of  $\text{Et}_3\text{B}$  (25  $\mu\text{L}$ , 0.025 mmol, 1 M in  $\text{CH}_2\text{Cl}_2$ ) and dry air (2 mL). Addition of  $\text{Et}_3\text{B}$ /air (25  $\mu\text{L}$ /2 mL) was repeated every 20 min, until reaction was judged completed by TLC. To the reaction mixture was then added *m*-dinitrobenzene, and the mixture was stirred for 15 min at  $-78^\circ\text{C}$ , followed by addition of a saturated aqueous solution of  $\text{NaHCO}_3$  and dilution with ether. The mixture was then warmed to rt, and the phases were separated. The aqueous phase was extracted with ether ( $\times 2$ ), and the combined organic fractions were dried over  $\text{MgSO}_4$  and concentrated under reduced pressure.

**C. Radical Reduction in the Presence of MAD.** To a solution of 2,6-di-*tert*-butyl-4-methylphenol (66 mg, 0.30 mmol) in  $\text{CH}_2\text{Cl}_2$

or toluene (0.5 mL) was added  $\text{Me}_3\text{Al}$  (75  $\mu\text{L}$ , 0.15 mmol, 2 M in hexane) at rt. Gas evolution was observed. The resulting solution (pale yellow or colorless) was stirred for 1 h at rt and was then cooled to  $-78^\circ\text{C}$ . A solution of the ester (0.10 mmol) in  $\text{CH}_2\text{Cl}_2$  or toluene (0.5 mL) was added to it via canula, followed by  $\text{Bu}_3\text{SnH}$  (54  $\mu\text{L}$ , 0.20 mmol) and  $\text{Et}_3\text{B}$  (25  $\mu\text{L}$ , 0.025 mmol, 1 M in  $\text{CH}_2\text{Cl}_2$ ). Addition of  $\text{Et}_3\text{B}$  (25  $\mu\text{L}$ ) was repeated every 20 min, until the reaction was judged completed by TLC. To the reaction mixture was then added *m*-dinitrobenzene, and the mixture was stirred for 10 min at  $-78^\circ\text{C}$ , followed by addition of a saturated aqueous solution of  $\text{NaHCO}_3$  and dilution with ether. The mixture was then warmed to rt, and a saturated aqueous solution of  $\text{Na}^+/\text{K}^+$  tartrate (5 mL) was added to facilitate the separation. The phases were separated, the aqueous phase was extracted with ether ( $\times 2$ ), and the combined organic fractions were dried over  $\text{MgSO}_4$  and concentrated under reduced pressure.

**Acknowledgment.** Y.G. thanks NSERC and IRCM for their generous funding. I.D. thanks Group Jean Coutu for a postdoctoral fellowship. J.C.S. thanks NSERC and CFI for generous funding of research and equipment. We further thank Dr. Keith Ingold for valuable comments on the ESR experiments.

**Supporting Information Available:** Experimental procedures for the preparation of **1**, **4**, **7**, **8**, and **13**; characterization data for **1–12**; proof of structure for **1**, **3**, **5**, **6**, and **9**; X-ray image for intermediate **S-5**. This material is available free of charge via the Internet at <http://pubs.acs.org>.

JO802634W